

Fatigue Crack Growth in Additive Manufactured Titanium: Residual stress control and life evaluation method development

Xiang Zhang¹, Filomeno Martina², Abdul Khadar Syed¹

Xueyuan Wang¹, Jiluo Ding², Stewart W Williams²

¹ *Coventry University, Faculty of Engineering, Environment & Computing, United Kingdom*

² *Cranfield University, School of Aerospace, Transport & Manufacture, United Kingdom*

Abstract: This paper presents fatigue crack growth behaviour in titanium alloy Ti-6Al-4V built by the Wire + Arc Additive Manufacture (WAAM®) process. Process induced residual stress and stress relief by cold working were measured by neutron diffraction and contour methods. Residual stress retained in the compact tension test specimens was evaluated by the finite element method based on the measured stresses in the WAAM wall. Fatigue crack growth rate in as-built and stress relieved conditions are discussed with respect of the effects of material build orientation, residual stress, and microstructure characteristics. Key conclusions are: (a) residual stresses arising from the WAAM process can be controlled and reduced significantly by cold working. Residual stress retained in compact tension specimens is low, resulting in low residual stress intensity factor. (b) Microstructure affects fatigue crack growth rate in two different material's build orientations. (c) Fatigue crack growth rate in WAAM Ti-6Al-4V is lower than that in traditional wrought plate, with and without the residual stress relief. Therefore, WAAM is a viable additive manufacture process to produce aerospace titanium alloys for damage tolerance design.

INTRODUCTION

Ti-6Al-4V (Ti-6-4) titanium alloy has been used in the aerospace industry owing to its high strength, excellent resistance to fatigue, corrosion and elevated temperature, and good compatibility with carbon fibre composites that are increasingly used in the airframes of new generation commercial aircraft. Since titanium is very expensive and difficult to machine, building parts by additive manufacture (AM) has become very attractive owing to the significant reduction in the costs of material and tooling, as well as the machining time and effort. Powder bed fusion technologies also have the advantages of building complex shapes and geometry freedom [1]. AM can be an economically and environmentally superior option to the traditional methods of machining from cast or forged billets [2,3].

This paper focuses on the Wire + Arc Additive Manufacture (WAAM®) process that works by feeding a wire at controlled rate into an electric arc to melt the wire onto a substrate or previously deposited layers. Compared with powder-based AM methods, the key advantage of WAAM is that it can produce large, near net shape parts with a deposition rate of several kilograms per hour, at acceptable cost and in reasonable times [4,5].

One of the main barriers to the widespread application of additive manufacture to aerospace components is the lack of systematic knowledge of the mechanical properties, particularly the fatigue and fracture response under the service load conditions, which are a key requirement for product qualification and certification, especially for flying parts. To date, there are a number of published works on the high cycle fatigue and fatigue crack growth behaviour in powder based AM titanium alloys [e.g. 6-11] and also wire based AM titanium [12]. In the four AM processes reported in the open literature (i.e. EBM, LENS, SLM, and WAAM), AM produced Ti-6-4 alloys show slower or comparable crack growth rates with reference to wrought plates or sheets. This is true for all the four processes, although SLM Ti-6-4 must be heat treated to relieve residual stresses, and eliminate defects such as lack-of-fusion or porosity, in order to have the comparable crack growth rate. On the other hand, previous research on WAAM Ti-6-4 shows that cold working (rolling) can improve the microstructure, static strength and reduce the residual stresses [13-15].

On the wire based AM processes, research has been performed by the authors on various aspects of fatigue and fracture performance of WAAM Ti-6-4 aiming at controlling the residual stress and developing qualification methods for this new material class under the fatigue loads for airframe applications. Our work has included the following aspects: (a) fatigue crack initiation from stress concentration sites, (b) fatigue crack growth (FCG)

behaviour, (c) residual stress relief by in-process cold working, and (d) developing FCG life prediction methods. In this paper, only the fatigue crack growth behaviour will be reported owing to the page limit. This includes the fatigue crack growth rate and crack propagation path under constant amplitude loads. Finite element analyses were performed to study the effect of material anisotropy on the stress intensity factor due to the applied load and the stress intensity caused by the AM process induced residual stress. Experimental test results are analysed in the light of residual stress and microstructure analysis.

METHODS

Experimental

WAAM walls of 8 mm nominal thickness were built by single pass WAAM process deposition on to a wrought material baseplate, Figure 1a. Residual stresses induced by the additive manufacturing process have caused out-of-plane distortion, Figure 1(b). All walls were machined and polished on both faces to remove surface roughness before extracting test specimens. After machining and polishing, the thickness was 5 mm.

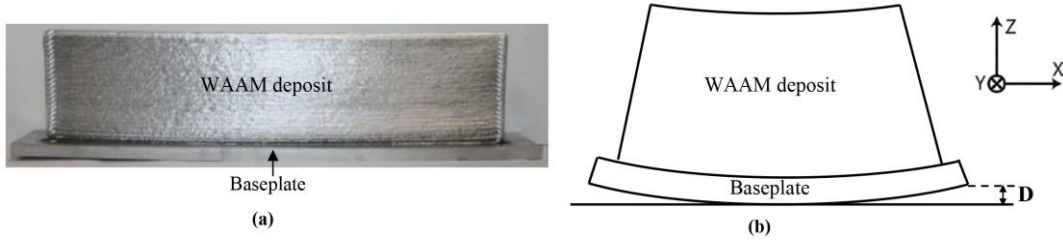


Figure 1. (a) A WAAM wall showing deposited layers built on a wrought material baseplate; (b) schematic of out-of-plane distortion as the consequence of residual stresses in WAAM process.

Four compact tension, C(T), specimens were extracted from each wall. Specimen orientation is defined according to the starter crack orientation with respect to the WAAM deposited layers. Two specimens have initial crack along the additive layers and two with crack across the layers as show in in Figure 2a. Geometry and dimensions of C(T) specimen are shown in Figure 2b. Thickness of all C(T) specimens is 5 mm and the characteristic width (W) is 70 mm that is the distance from the loading hole centre line to the specimen edge and is often quoted for the C(T) geometry.

Residual stress in WAAM walls was evaluated using the neutron diffraction method. Details can be found in [16] and key results are summarised in the following section. Residual stress retained in the C(T) specimens extracted from the walls were measured by the contour method. Microstructure characterisation was performed by optical microscope and scanning electron microscope (SEM). Effect of microstructure on crack propagation rate and crack path is discussed in next section.

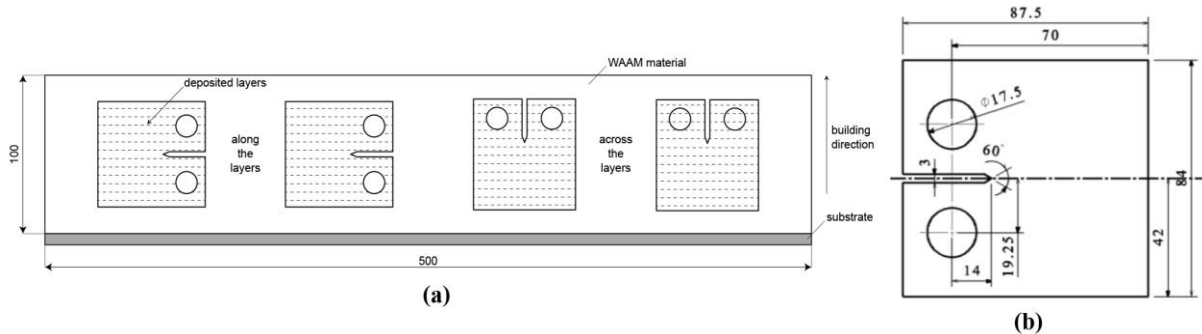


Figure 2. (a) Schematic of extracting C(T) specimens from a WAAM wall; two crack orientations: crack growth along the additive layers (left) and crack across the layers (right). (b) details of C(T) specimens used for fatigue crack growth tests (unit: mm; thickness = 5 mm).

Finite element analysis

Finite element analysis (FEA) was performed to evaluate (a) retained residual stresses in the C(T) specimens based on the measured of residual stresses in the WAAM wall, (b) the influence of material anisotropy, i.e. the difference in the elastic modulus between the two build orientations, on the crack tip stress intensity factor (SIF). Other mechanical properties, e.g. the yield strength and ductility, are also direction dependent. However, they will not affect the stress intensity factor values using the theory of linear elastic fracture mechanics.

RESULTS

Residual stress analysis

Residual stress in WAAM wall and stress relief by cold rolling. Residual stresses in WAAM walls built on a baseplate in as-built and cold rolled conditions with rolling force of 50 or 75 kN were measured and shown in Figure 3. Neutron diffraction method was used for the measurement [16]. Peak residual stress in the as-built condition is about 500 MPa. Residual stress is significantly reduced to below 300 MPa by applying a rolling force of 50 to 75 kN (Figure 3).

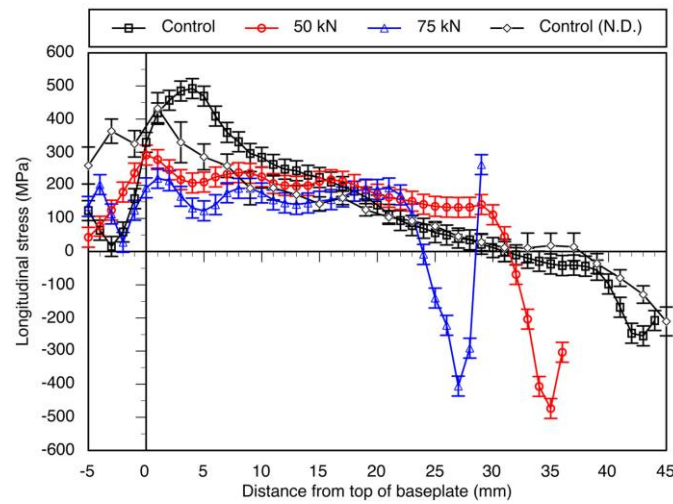


Figure 3(a). Longitudinal residual stress measured by contour method and comparison with the neutron diffraction (N.D.) measurements of the control sample [16].

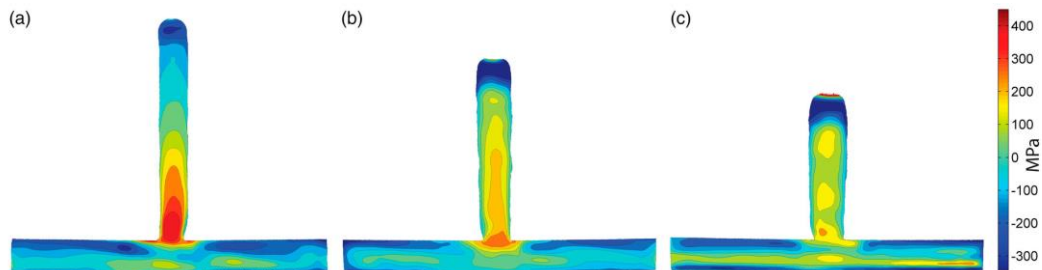


Figure 3(b). Contour maps of residual stress for the same case in Figure 3a: (left): control; samples rolled using the profiled roller with a load of 50 kN (middle) and 75 kN (far right) [16].

Residual stresses retained in C(T) specimens. Residual stress profile in another as-built WAAM wall is shown in Figure 4. The height of the WAAM part is 110 mm, and without in-process cold working. The stress is in the longitudinal direction of the wall that is the welding torch movement direction. The stress was measured by the contour method [17] as well as calculated by thermal mechanical FE analysis [18].

Some of the C(T) specimens presented in this paper were extracted from the “as-built” walls of 145 mm height with residual stress profile like those shown in Figure 4. Some of the residual stress will be released when extracting smaller C(T) specimens from the WAAM wall. This is owing to the material removal process when extracting smaller C(T) specimens from the wall. The magnitude and distribution of retained residual stresses in C(T) specimens were evaluated by FEA [14]. The FE model of the wall and C(T) specimen locations are shown in Figure 5. The geometry and dimensions of C(T) specimens are the same as Figure 2b, and the positions of the specimen types AL (across layers) and PL (parallel to layers) are shown in Figure 5. Solid elements (second order element designated as C3D20 in ABAQUS) were used to mesh the model. The size of element is $3 \times 3 \times 3$ mm³. Young’s modulus of 113.8 GPa and Poisson’s ratio of 0.34 are used for the material properties. Boundary conditions just constrain the rigid body movement but allow deformation in any direction to simulate the specimen extraction process. The longitudinal residual stress shown in Figure 4 was applied to whole area of FE

model of the wall by using the SIGINI subroutine. After removing the elements surrounding the C(T) specimens, residual stresses along the crack path from the notch root were found as shown in Figure 6.

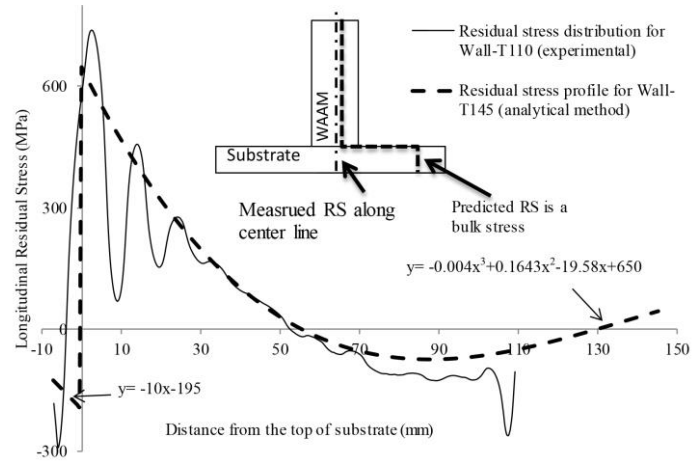


Figure 4. Residual stress profiles in a WAAM wall and baseplate (substrate) evaluated by the contour method (experimental) and also thermal mechanical analysis [18].

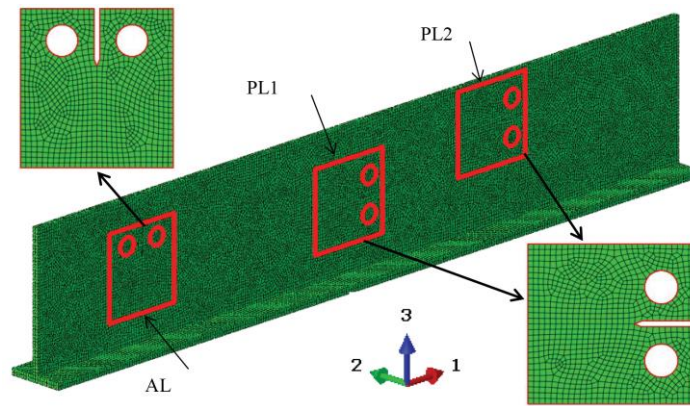


Figure 5. Finite element models of a WAAM wall and extraction of several C(T) specimens of two crack orientations [18].

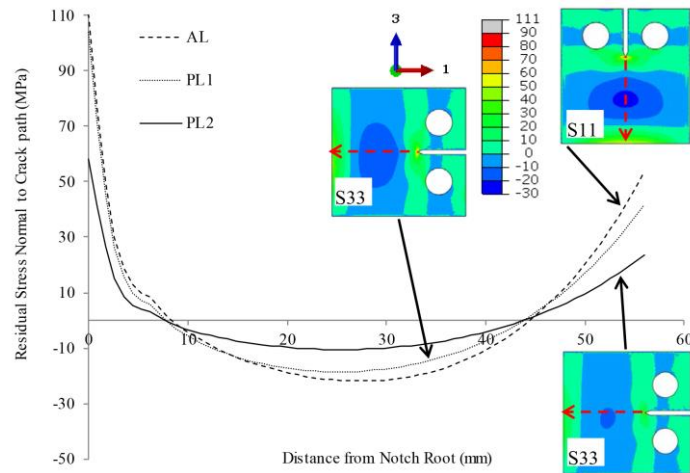


Figure 6. Residual stress profiles in C(T) specimens of two different orientations. In this figure, AL means crack across layers, PL means crack parallel to layer, i.e. along layers [18].

Stress intensity factor calculations

Crack growth driving force the stress intensity factor (K_{total}) resulting from the applied load (K_{app}) and residual stress (K_{resid}). FE analysis using two different Young's modulus in the two major directions with respect to the WAAM build direction shows that with a difference of 5.6% in the elastic modulus, the calculated K_{app} is within 1% over a crack length range of 17 to 56 mm [18]. In terms of the crack growth driving force SIF, effect of material anisotropy in the additive manufactured titanium is very small. Therefore, isotropic material properties are used in the fracture mechanics analysis in this study.

Stress intensity factors owing to the *residual stress* in two crack orientations were also calculated by FEA using two specimen types: crack growth across the layers (denoted as AL specimen in [18]), and crack growth in parallel to the layers (PL specimen). Two-dimensional plane stress elements were used to simulate the stress intensity factors in the specimens. Residual stress field was applied to the FE model of WAAM wall by directly inputting the corresponding residual stress values to the wall model. C(T) specimen extraction was modelled by material removal. The crack tip stress intensity factors due to residual stress, K_{res} , were obtained by subtracting K_{app} from the K_{tot} . Calculated SIF (K_{res}) are shown in Figures 7 and 8 for the two crack orientations, AL and PL.

Residual stress intensity factor (K_{res}) is small with the highest value being 5.5 MPa√m at the notch tip. For the PL specimen, there is a small amount of mode II K_{res} , about 0.5 MPa√m, owing to the unsymmetric distribution of residual stress with respect to the crack centre line. The value of K_{res} also depends on the position where the C(T) is extracted, as shown in Figure 8, i.e. 28 or 67 mm from the interface of WAAM wall with the baseplate.

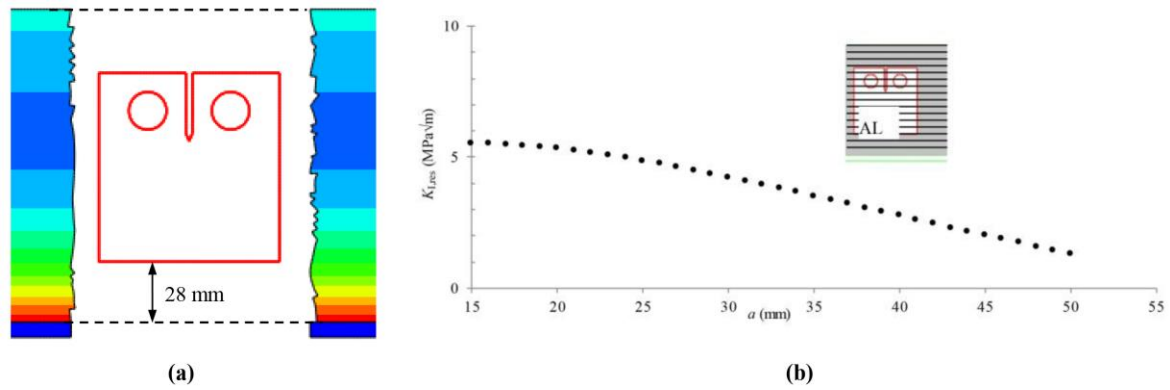


Figure 7. Crack growth across the additive layers (defined as “AL” specimen in [13]): (a) positions of C(T) specimen FE model in residual stress field of the WAAM wall model (indicated by colour stress maps on both side of the CT), (b) calculated mode I stress intensity factor due to residual stress in the C(T) [18].

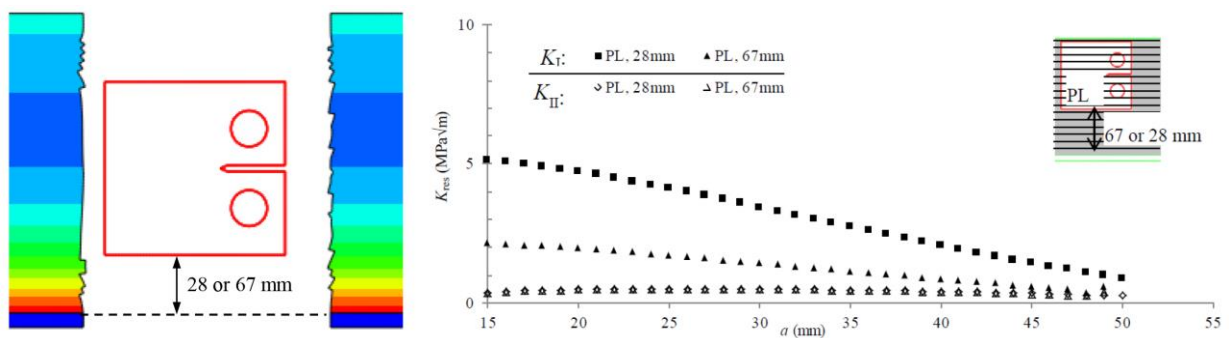


Figure 8. Crack growth in parallel to the additive layers (“PL” specimen = crack along the layers): (a) positions of C(T) specimen FE model in measured residual stress field of the WAAM wall (indicated by colour stress maps on both side of the CT model), (b) FE calculated mode I and mode II stress intensity factors due to residual stress in the C(T), which has two positions, 28 or 67 mm from the baseplate [18].

Fatigue crack growth rates (FCGR)

Measured fatigue crack growth rates are shown in Figure 9 for as-built WAAM and compared with two reference materials produced by traditional manufacture methods, wrought and cast Ti-6-4.

Direction dependent material properties found in the static load tests was found having negligible effect on the crack tip stress intensity factor. Residual stress influence is also small owing to stress release after extracting small C(T) specimens from the wall. Therefore, the difference in fatigue crack growth rate between the two crack orientations is ascribed to the microstructure difference. Two observations are made:

a) The layer banding appearance shows a systematic and repetitive variation in the size of the α lamellae along the build direction, resulting in more resistance to crack propagation across the layers (AL) than crack being along or parallel to the layers (PL). For the AL type specimens, a propagating crack tip encounters the continuous variation of the α lamellae size that should slow down the crack growth rate, Figure 10. However, the longitudinal residual stress is perpendicular to the crack plane, increasing the crack growth driving force with resulting K_{res} being about 5 MPa \sqrt{m} . The interaction has resulted in similar crack growth rates in the two crack orientations in the geometry and size tested (Figure 9). Crack across the layer has slower growth rate when ΔK_{app} is lower than 20 MPa \sqrt{m} owing to the effect of microstructure. Microstructure effect on FCGR disappears when crack is longer. In this study it is when ΔK_{app} is greater than 20 MPa \sqrt{m} .

b) Figure 9 also shows that wrought alloy's FCGR is greater than that of the WAAM, and the cast alloy has the slowest FCGR. The reason is also the microstructure difference; crack growth path in wrought (a fine equiaxed grain structure) is straight and smoother than in WAAM (a coarse lamellar grain structure), whereas cast Ti-6-4 has coarse lamellar grain structure that is similar to the WAAM Ti-6-4 tested in this study.

Effect of in-process cold work on crack growth rate. Fatigue crack growth rates (FCGR) in the cold worked specimens (rolling force 75 kN) are shown in Figure 11. Two crack orientations were studied by testing two specimens in each case: crack across layers and crack along the layers. The following observations can be made. (a) For the rolled specimens: the difference between the two crack orientations is little except when ΔK_{app} is below 18 MPa \sqrt{m} . Under constant amplitude load, this means the crack being small, so the grain structure is making the difference as discussed around Figure 10 for the as-built specimens. (b) The difference in FCGR between the rolled and the as-built specimens (Figure 9) is also small because the rolled samples were tested at a higher stress ratio $R = 0.5$, whereas the as-built samples were tested at $R = 0.1$. For a given applied SIF range (the x -axis), higher stress ratio means higher mean stress; hence greater crack growth rate. However, the rolled samples at $R = 0.5$ had almost the same crack growth rates as the as-built at a much lower R ratio. Therefore, it can be said that in-process rolling has effectively reduced the crack growth rate owing to reduced residual stresses (Figure 3), and also owing to the superior mechanical performances (higher proof and ultimate strengths) that is reported in the literature [13-15].

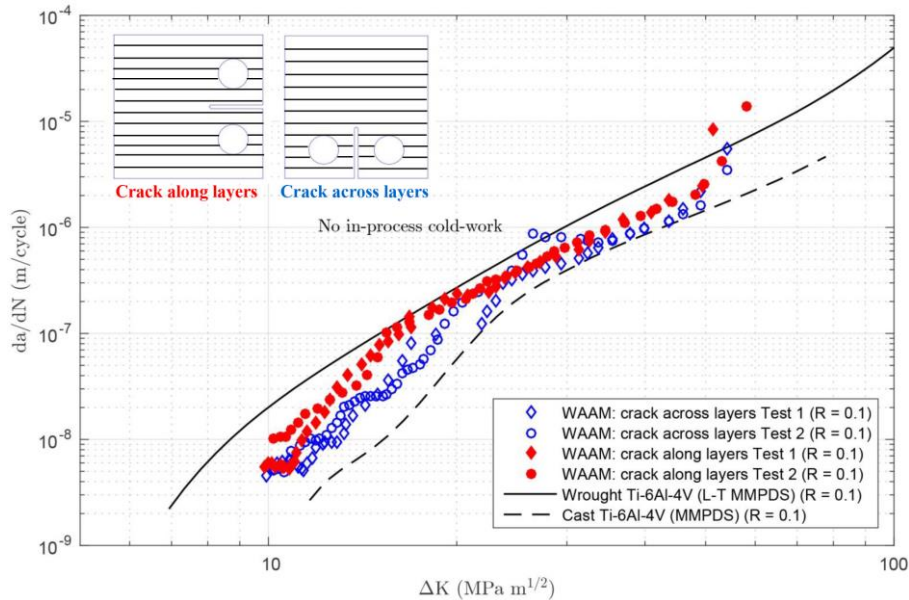


Figure 9. Crack growth rate in as-built specimens; two tests in each case.

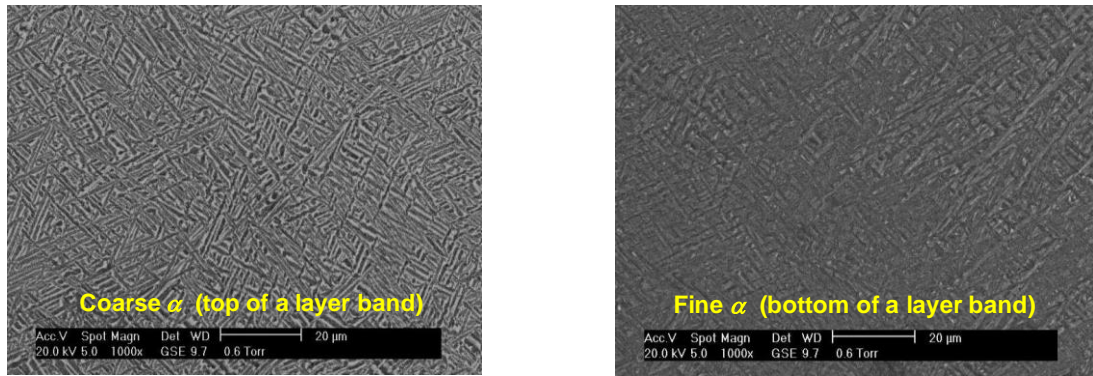


Figure 10. Microstructure of WAAM Ti-6-4: (a) upper part, (b) bottom part of a layer band

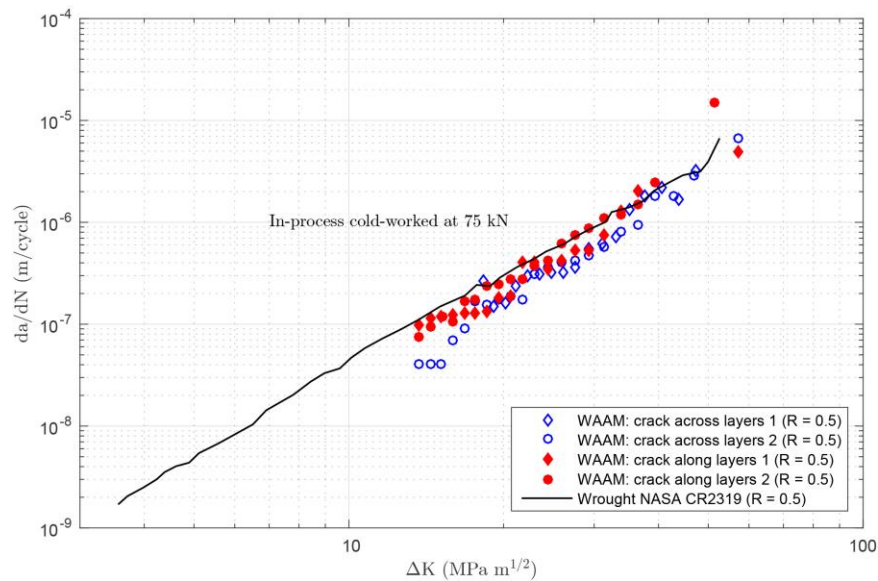


Figure 11. Crack growth rate in rolled specimens (two tests each case) and reference wrought material.

ACKNOWLEDGEMENT

The work was performed with support of the WAAMMat programme industrial partners. Financial support from the Engineering and Physical Sciences Research Council (Grant No EP/K029010/1) is acknowledged. Authors thank Xudong Qui for conducting part of the experiments. Enquiries for access to the data referred to in this article should be directed to researchdata@cranfield.ac.uk.

CONCLUSIONS

- Residual stress in WAAM walls can be relieved significantly by the in-process rolling process.
- Residual stress retained in the C(T) specimens of 84 x 84 mm size is low owing to stress release when extracting the test specimen from the WAAM wall. This has led to low value of residual stress intensity factor.
- Fatigue crack growth rate (FCGR) in WAAM Ti-6Al-4V is slower than that of reference wrought plates. Therefore, for damage tolerant design, WAAM appears to be a viable candidate manufacturing process.
- Microstructure effect causes direction dependent crack growth rate, which is slower when crack propagates across the additive build layers comparing to crack growing along the layers. However, the difference is small.
- FE model presented in this study can account for the effects of material anisotropy, material orientation and residual stress, which can be further developed for damage tolerance analysis of additive manufactured metals.

REFERENCES

- [1] Thompson, M.K., Moroni, G., Vaneker, T., Fadel, G., Campbell, R.I., Gibson, I., Bernard, A., Schulz, J., Graf, P., Ahuja, B., Martina, F. (2016). *CIRP Annals Manufacturing Technology*, vol 65(2), pp. 737–760.
- [2] Brandl, E., Leyens, C., Palm, F. (2009). *Trends in Aerospace Manufacturing, 2009 Intl Conference*. IOP Conf. Series: *Materials Science and Engineering*, vol. 26 (2011).
- [3] Herzog, D., Seyda, V., Wycisk, E., Emmelmann, C. (2016). *Acta Materialia*, vol. 117 pp. 371-39.
- [4] Martina, F., Mehnen, J., Williams, S.W. et al. (2012). *J. Mater. Process Technol.* vol. 212, pp. 1377-86.
- [5] Wang, F., Williams, S.W., Rush, M. (2011). *Int J Adv Manuf Tech.* vol. 57, pp. 597-603.
- [6] Edwards, P., O’Conner, A., Ramulu, M. (2013). *J Manufact Sci & Engng*, vol. 135, pp. 061016/1-7.
- [7] Van Hooreweder, B., Moens, D., Boonen, R. et al. (2012). *Adv Engng Mater*, vol. 14, pp. 92-97.
- [8] Leuders, S., Thöne, M., Riemer, A., Niendorf, T., et al. (2013). *Int J Fatigue*, vol. 48, pp. 300-307.
- [9] Zhai, Y., Lados, D.A., Brown, E.J., et al. (2016). *Int J of Fatigue*, vol. 93, pp. 51-63
- [10] Riemer, A., Richard, H.A. (2016). *Procedia Structural Integrity*, vol. 2, pp. 1229-36.
- [11] Donoghue, J., Antonysamy, A.A., Martina, F., Colegrove, P.A., Williams, S.W., Prangnell, P.B. (2016). *Materials Characterization*, vol. 114, pp. 103–114.
- [12] Zhang, X, Martina F, Ding J, Wang X, Williams S. (2016). *Fatigue & Fracture of Eng Mater & Struct*.
- [13] Martina, F., Colegrove, P.A., Williams, S.W., Meyer, J. (2015). *Metallurgical and Materials Transactions A*, vol. 46, n. 12, pp. 6103–6118.
- [14] Szost, B., Terzi, S., Martina, F., Boisselier, D., Prytuliak, A., Pirling, T., Hofmann, M., Jarvis, D.J. (2015). *Materials & Design*, vol. 89, pp. 559–567.
- [15] Lu, S., Bao, R., Wang, K., et al. (2017). *Materials Science & Engineering A*. vol. 690, pp. 378-386.
- [16] Martina, F., Roy, M. J., Szost B. A., et al. (2016). *Mater Sci & Tech*, vol. 32, n. 14, pp. 1439-1448.
- [17] Paddea, S. (2014). Technical report (unpublished), Open University, UK
- [18] Wang, X. (2017). PhD Thesis, Coventry University, UK.

2017-06-09

Fatigue crack growth in additive manufactured titanium: residual stress control and life evaluation method development

Zhang, Xiang

VTT Information Service

Zhang X, Martina F, Syed AK, et al., (2017) Fatigue crack growth in additive manufactured titanium: residual stress control and life evaluation method development. In: ICAF 2017 35th ICAF Conference and 29th ICAF Symposium, 5-9 June 2017, Nagoya, Japan

<https://dspace.lib.cranfield.ac.uk/handle/1826/15165>

Downloaded from Cranfield Library Services E-Repository